Enhancing Traveling-Wave Dielectrophoresis with Signal Superposition

A New Method for Cell Separation and Characterization and for Monitoring Cell Physiological Changes

RONALD PETHIG, MARK S. TALARY, AND RICHARD S. LEE

The modes of interaction of biological particles (such as cells, bacteria, viruses, DNA, and proteins) with alternating current (ac) electric fields is an active area of investigation, with potentially important uses in medical diagnostics, drug discovery, and cell therapeutics, as well as emerging biothreat applications. The desired objective in many cases is to use electric fields to selectively isolate, concentrate, or purify target bioparticles when present in suspensions of mixed particles. Examples include the isolation of stem cells, fetal cells, cancer cells, or bacteria from blood for therapy or further analysis.

Masuda et al. [1] applied a traveling electric field, produced by applying poly-phase voltages to a parallel array of electrodes, to an aqueous suspension of blood cells. They found that they could control both translational and circular motions of the cells. The optimal frequency range for such motions was found to be 0.1–10 Hz. As is to be expected when working at such low frequencies, these induced cell motions were largely electrophoretic in origin and dependent on cell size and electrical charge carried by the cells. Hagedorn et al. [2] later demonstrated that quadrature-phase electric fields of frequency between 10 kHz and 30 MHz could produce linear motions of pollen and cellulose particles. At these higher frequencies the influence of field-induced dipole moments is more important than particle surface charge, and dielectrophoresis (DEP), rather than electrophoresis, is the dominant phenomenon. Hagedorn et al. [2] coined the term traveling-wave dielectrophoresis (TWD) for this motion and found that TWD was restricted to a frequency range where the particles were levitated above the electrodes under the influence of a negative DEP force. This finding was confirmed by Huang et al. [3] who further deduced that the TWD velocity was proportional to the imaginary (out-of-phase) component of the induced dipole moment, with the DEP levitational force being proportional to the real (in-phase) component.

Theoretical models of TWD have been refined [4]–[6] and various practical devices have been developed for manipulating, separating, and characterizing blood cells, cancer cells, yeast, and parasites [7]–[12]. By employing TWD it is possible to selectively move cells or other bioparticles along a channel in a stationary fluid. Selective movement arises from the intrinsic physico-chemical properties of the bioparticle. In many cases tagging the target particle with a biochemical label, bead, dye, or other bioengineered marker is not required to achieve selective isolation of the target from other particle types. TWD electrodes can be fabricated in the form of spirals [8], [9], tracks [10], and junctions [11]. Dense concentrations of cells, as well as single cells, can be manipulated and sorted [12]. Provided that sufficiently long TWD electrode tracks are used, a mixture of different particles can be fractionated into "bands" with a high degree of separation [10], [12].

The studies described above apply to the situation where the particles are exposed to one traveling-wave signal. In this article we describe and give examples of how the sensitivity and utility of TWD cell separations can be enhanced by superimposing one or more traveling-wave and standing-wave signals of different frequencies onto an electrode array [13]. An important advantage of using superimposed traveling waves is that bioparticle separations of improved sensitivity and purity can be achieved on much smaller devices, facilitating their integration into miniaturized instrumentation and automated lab-on-a-chip technologies.

Theoretical Modeling

Figure 1 depicts an array of interdigitated electrodes suitable for generating both traveling and standing electrical waves. Such electrodes commonly consist of thin layers of gold, deposited onto a planar insulating substrate such as glass, and fabricated by photolithography or excimer laser ablation. In this figure the width d of each electrode is the same as the gap between electrodes, but this does not always have to be the case. Also, the electrodes need not take the form of straight-sided, parallel, bars.

A traveling ac field can be generated by sequentially addressing the electrodes with sinusoidal voltages of the same frequency, and with a phase difference of 90° between consecutive electrodes as shown in Figure 1. The direction of propagation is toward the smaller phase regions. Reversing this quadrature phase sequence causes the direction of wave propagation to reverse. The traveling wave has a wavelength λ equal to the distance between every fourth electrode, so that for the case shown in Figure 1, $\lambda = 8d$. For DEP, the electrodes are connected alternately to two sinusoidal voltages of the same frequency with phases of 0° and 180°. This creates a stationary ac field.

0739-5175/03/$17.00©2003IEEE

An important advantage of using superimposed traveling waves is that bioparticle separations of improved sensitivity and purity can be achieved on much smaller devices.

The time-averaged DEP force acting on a particle arises from the interaction of the induced dipole moment with the applied field phasor. This is summarized for a particle of radius r suspended in a medium of permittivity ε_m by the following equation [8]:

$$F = 2\pi\varepsilon_m r^3\{\mathrm{Re}(m)\nabla E^2 + \mathrm{Im}(m)\Sigma E^2\nabla\phi\} \quad (1)$$

∇E^2 is the gradient of the square of the applied field E, and $\Sigma E^2\nabla\phi$ represents a summation involving the magnitude and phase ϕ of each field component in a Cartesian coordinate frame. The polarizability factor m determines the magnitude of the induced dipole moment and is a function of the frequency of the applied field and the conductivity and permittivity of the particle and its suspending medium. Re(m) and Im(m) relate to the real (in-phase) and imaginary (out-of-phase) components of this dipole moment, respectively. Re(m) is bounded by values of +1 and −0.5, and Im(m) falls within the bounds of +0.75 and −0.75. Values for Re(m) and Im(m) can be determined using the so-called multishell model of a cell, further details of which are given elsewhere [3], [8]. Figure 2 shows the frequency dependencies of these two parameters for human monocytes and T lymphocytes, using a three-shell model that takes into account the properties of the nucleus, cytoplasm, outer membrane, and surrounding electrolyte. The relevant dielectric and physical properties of these cell types were derived from measurements using Aura's Cell Physiometry™ technology [14].

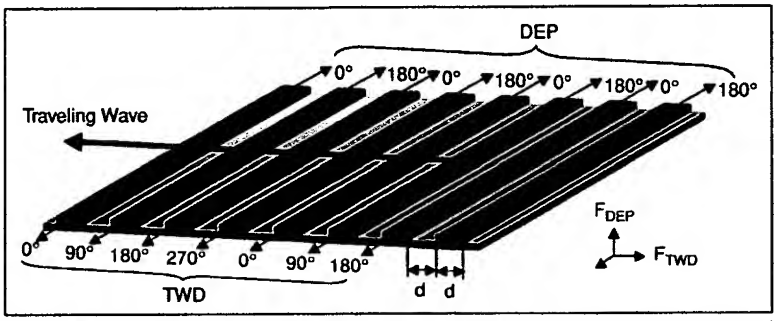

Fig. 1. Diagram showing the electrical phase connections applied to an array of electrodes to produce both a DEP and a TWD force on particles suspended above the electrode plane. The DEP force (F_{DEP}) acts either to levitate the particles or to attract them to the electrode edges. The TWD force has a vertical component that acts in the same manner as a DEP force, as well as a horizontal component (F_{TWD}) that can induce translational motion of particles along the electrode track.

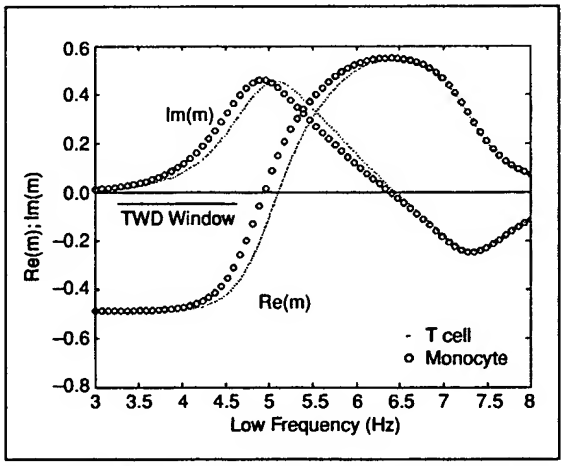

Fig. 2. Variations of the real (Re(m)) and imaginary (Im(m)) components of the polarizability factors in (1) as a function of frequency, modeled for the case of human monocytes and T cells suspended in an aqueous medium of conductivity 40 mS/m. TWD motion occurs when the particles are levitated above the electrode plane (i.e., Re(m) must be negative) and when Im(m) has a value of sufficient magnitude to generate a translational TWD force.

For the DEP case, where the electrodes are energized with the two phases of 0° and 180°, a stationary field is generated with no spatially varying phase. In this case the factor $\Sigma E^2\nabla\phi$ in (1) is zero. The resulting DEP force acts to either levitate the particle or to attract it to the electrode edges, depending on the sign of Re(m). This DEP force has no component acting along the electrode array, and so no translational movement of the particle occurs. When the electrodes are energized with the quadrature phases (0°, 90°, 180°, and 270°) a traveling field is generated, having a spatially dependent phase. The total DEP force now consists of a component (Re(m)∇E^2) normal to the electrode plane, and a component (Im(m)$\Sigma E^2\nabla\phi$) directed along the electrode track. The direction and velocity of the induced TWD motion along the track depends on the magnitude of the phase gradient factor $\Sigma E^2\nabla\phi$ and on the magnitude and sign of Im(m). As shown in Figure 2, the frequency range over which TWD motion occurs is defined by the situation where the cells are levitated above the electrodes by a negative DEP force (i.e., Re(m) negative) and where Im(m) is of suffi-

If a DEP or second TWD signal is added to the first TWD signal, the resulting electrostatic potential at the electrodes will be a superposition of the separate voltage functions.

cient magnitude to generate a translational TWD force.

The magnitudes of ∇E^2 and $\Sigma E^2 \nabla \phi$, modeled using the 3D Electromagnetic Field Simulator (Ansoft, Pittsburgh, Pennsylvania) are shown in Figure 3 as a function of height above the electrode plane. These results show that as a particle approaches the electrode plane, a strong DEP force directs it toward the electrode edges and the TWD force reverses in polarity. The same forms of variations of ∇E^2 and $\Sigma E^2 \nabla \phi$ have been derived using the charge density method [5], Green's theorem [8], finite-element mesh method [15], and Fourier series analysis [6]. These various methods of analysis indicate that TWD takes the form of simple translational motion for particles levitated higher than d above the electrode plane. When particles approach the electrodes, they can exhibit circular and spinning motions as well as sudden reversals in their direction of travel. Such effects were noted in earlier studies [3] and designated as the FUN (fundamentally unstable) regime.

For levitation heights greater than d, the time-averaged TWD velocity is given by the following expression [8]:

$$v_{TWD} = -\frac{\varepsilon_m r^2 V^2}{3\eta} \mathrm{Im}(m) \Sigma E^2 \nabla \phi \qquad (2)$$

in which η is the viscosity of the suspending electrolyte and V the applied (rms) voltage. For an aqueous electrolyte we have $\varepsilon_m \sim 7 \times 10^{-10}\ \mathrm{F \cdot m^{-1}}$ and $\eta \sim 10^{-3}\ \mathrm{kg \cdot m^{-1} \cdot s^{-1}}$. For the case of a lymphocyte ($r \sim 5\ \mu\mathrm{m}$) levitated to a height of 25 μm on applying a 1 Vrms signal, and assuming $\mathrm{Im}(m) \sim 0.6$, then from Figure 2 and (2) we obtain an anti-field TWD velocity of $\sim 22 \mu\mathrm{m \cdot s^{-1}}$. Particle velocity values of this order are typically observed in TWD experiments [3], [7], [8], [13]. As discussed by Wang et al. [8] the TWD velocity increases with increasing applied voltage but not as a voltage-squared dependency as suggested by (2). With increasing voltage the increased DEP force causes an increase of particle levitation height, and, as shown in Figure 3, this leads to a smaller value for $\Sigma E^2 \nabla \phi$ for levitation heights greater than 15 μm.

If a particle is assumed to be in the far-field region, way above the electrode plane, where the field and DEP force decay exponentially as a function of levitation height, the following voltage-independent expression can be derived for the TWD velocity [6]:

$$v_{TWD} = \frac{2}{9} \frac{r^2 \Delta \rho g}{\eta} \frac{\mathrm{Im}(m)}{\mathrm{Re}(m)} \qquad (3)$$

where $\Delta\rho$ is the difference between the specific densities of the particle and suspending electrolyte, and g is the gravitational acceleration factor ($9.81\mathrm{m \cdot s^{-2}}$). For lymphocytes suspended in an aqueous electrolyte, $\Delta\rho$ has a value $\sim 0.04\ \mathrm{kg \cdot dm^{-3}}$. For $\mathrm{Re}(m) = -0.4$ and $\mathrm{Im}(m) = 0.6$, (3) predicts an anti-field TWD velocity of $\sim 3.3\ \mu\mathrm{m \cdot s^{-1}}$ for lymphocytes. In the work reported here, the TWD velocities are considerably larger than this value and are voltage dependent. This indicates that in our experiments we are operating under conditions where (2) rather than (3) is pertinent.

If a DEP or second TWD signal is added to the first TWD signal, the resulting electrostatic potential at the electrodes will be a superposition of the separate voltage functions. Provided that nonlinear effects are absent, such as those arising from electrode polarization, high power dissipation, or a frequency variation of ε_m, for example, there will be a linear superposition of the effects caused by these two signals [13]. The total resultant DEP and TWD force acting on a cell will be the vector sum of the individual forces produced by each signal acting separately. We use the expression "superposition TWD" to describe this effect.

The stable levitation height h of the cell above the electrode plane is thus determined by the balance between the gravitational force and the sum of the vertical components

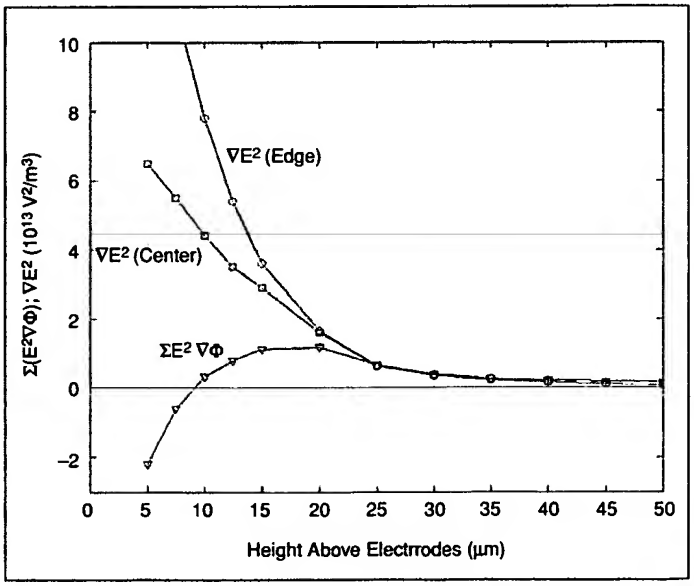

Fig. 3. Variations of ∇E^2 and $\Sigma E^2 \nabla \phi$ as a function of height above the electrode array shown in Figure 1, with $d = 10\ \mu$m and an applied phase quadrature signal of 1 V.

of the DEP and TWD forces. These various force components are all dependent on particle volume, so that particles with the same dielectric properties and density but different sizes can be expected to levitate to the same height—as is the case for DEP field-flow fractionation [15], [16]. On the other hand, particles with differing dielectric properties will levitate to different heights above the electrode plane irrespective of their size. Equations for determining the stable levitation height have been formulated [6], [15], [16] for the simplifying case of the DEP and TWD forces decaying as a single exponential function of the height h above the electrode plane ($\exp(-\pi h/d)$ for DEP and $\exp(-\pi h/2d)$ for TWD). The DEP and TWD forces do not behave in this simple manner over the full range of possible heights, but it is a useful approximation for our present purpose. Our procedure to model superposition TWD thus takes the form of calculating the resultant vertical component of the sum of the DEP and TWD forces, calculating the stable levitation height, and from this the value of the factor $\Sigma E^2 \nabla \phi$ to be used in (2). Corrections can be made to take into account electrode polarization effects [15], [16] and attenuation of voltage magnitude along the electrode track, but these have not been applied in the models described here.

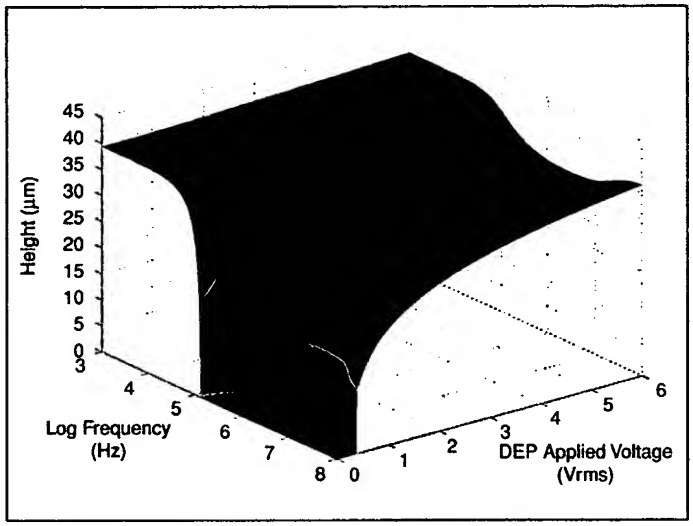

Fig. 4. Variation of the levitation height (microns) of T cells above the electrode plane as a function of the frequency of a 0.5 V(rms) TWD signal, and also as a function of the magnitude of a superimposed DEP signal of a fixed frequency of 10 kHz.

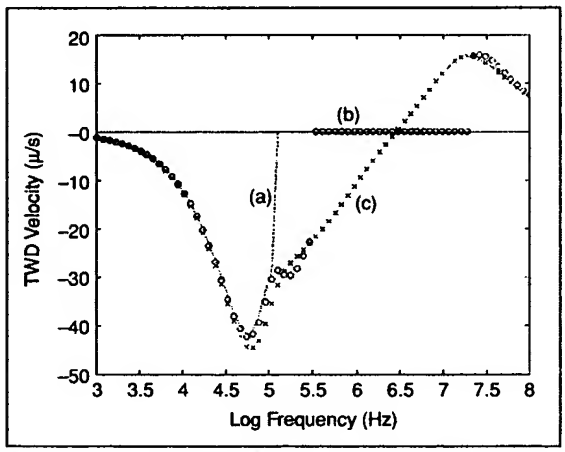

Fig. 5. Simulations of the TWD frequency spectra for human T lymphocytes for the case (a) of a pure traveling wave and (b), (c) a progressive increase in magnitude of a superimposed 10 kHz DEP signal. To avoid effects associated with the complex forms of the parameters ∇E^2 and $\Sigma E^2 \nabla \phi$ near the electrode plane, the TWD velocity is taken as zero for a levitation height less than 15 μm. The medium conductivity is 40 $mS \cdot m^{-1}$.

The effects of adding a 10 kHz DEP signal to a TWD signal are shown in Figures 4 and 5, for the case of T cells suspended in an aqueous electrolyte of conductivity 40 $mS \cdot s^{-1}$. The added DEP signal produces an additional levitation force that acts across the complete TWD frequency spectrum. As shown in Figure 4, the effect of this is to extend the range of frequencies over which the cells are levitated above the electrode plane, instead of being attracted to the electrodes under a net positive DEP force. For a small superimposed DEP signal, this results in the low-frequency window for counter-field TWD being extended to a higher frequency. As the DEP signal is progressively increased, a co-field TWD window first opens at the higher frequencies, and then, as shown in Figure. 5, TWD becomes operative across the full range of frequencies. This is shown more fully as a 3-D plot in Figure 6. For small magnitudes of the added DEP signal, a range of frequencies (marked as region "A" in Figure 6) exists where the cells are attracted to the electrodes. When this occurs, the cells often exhibit the so-called FUN effect [3], characterized by unstable motions that can include rotation as well as sudden reversals in their direction of TWD motion. Significant shear forces can be exerted on some types of cells during such behavior, and for large applied voltages these forces can be sufficient to irreversibly damage or burst the cells. Such selective cell bursting may be a desired objective, but more usually this is not the case and the electrical signals to the electrodes are programmed to avoid this regime.

Figure 7 shows the TWD spectra for T cells and monocytes modeled for the case of a superimposed 10 kHz DEP signal. At 40 kHz the T cells and monocytes exhibit anti-field TWD with velocities of 38 and 64 $\mu m \cdot s^{-1}$, respectively. At 1.3 MHz the T cells have an anti-field velocity of 9 $\mu m \cdot s^{-1}$, while the monocytes are trapped at the electrodes or exhibit effects associated with the FUN regime [3].

Experimental Methods

Cell Cultures

Human T lymphocytes (Jurkat E6-1) and monocytes (U-937) were obtained from American Type Culture Collection (ATCC: TIB-152 and CRL-1593.2, respectively) and kept in exponential growth as determined by doubling time. Cells were maintained in RPMI media containing Modified RPMI-1640

(ATCC) supplemented with 10% fetal bovine serum (ATCC), 100 U/mL penicillin, and 100 μg/ml streptomycin (Gibco/BRL). Cells were grown in a humidified incubator at 37°C, with 5% CO_2, 95% air.

Dielectrophoresis Experiments

Immediately before the experiments, cells were washed two times with 10 mL of an isotonic low conductivity media (ILCM) containing 8.6% w/w sucrose, 0.3% w/w dextrose, and 1.0 mg/mL BSA (Sigma), pH 7.4. The conductivity of the ILCM was adjusted to 40 mS/m at 25 °C, by adding modified Eagle's minimum essential media (ATCC) at a ratio of about 40:1, and using a YSI 3200 conductivity instrument with an Orion 018012 conductivity flow cell. After washing, the cells were suspended in the ILCM, and the osmolality of this cell suspension media remained near 296 mmol/kg, as determined using a Vapro 5520 vapor pressure osmometer.

The osmolality and conductivity of the suspension medium were checked before and after each experimental run. Two types of experiments were performed using our Cell Physiometry™ tools, namely a profiling of DEP characteristics using a PhysioNetics™ instrument [14] and Superposition-TWD cell manipulations using a CellNetics™ instrument. In both cases, the ILCM-cell suspensions were introduced into a chamber that is integrated within the instrument. These chambers contained microelectrode arrays fabricated using photolithography. For the PhysioNetics™ measurements, a sequence of ac voltages was automatically applied to the microelectrodes, and images of the DEP-induced motions of the cells were captured at 30 frames per second. The location and diameter of individual cells were continuously tracked, and one output of these measurements is a value of the so-called DEP cross-over frequency (DEP_{XO}) for individual cells. Further details are provided elsewhere [14]. Apart from representing a sensitive marker to characterize different cell types and changes in cell state [14], the value for DEP_{XO} corresponds to the upper frequency point where cells can exhibit translational motion when a single TWD signal is applied to the electrodes. Knowing the characteristic value of DEP_{XO} for different cell types provides guides as to how they will respond in the CellNetics™ instrument. In this instrument, DEP signals can be added in controlled ways to one or more TWD signals.

For some of the experiments T cells and monocytes were labeled with a fluorescent CD2-FITC (Leu™-5b) and CD33-PE (Leu™-M9) antibody (B D Immunocytometry Systems), respectively, in order to verify that separation of T cells from monocytes had been achieved by the TWD procedures described here.

Results

Figure 8 shows the TWD response for T lymphocytes as a function of the amplitude of a superimposed 10 kHz DEP signal. There is good agreement with the theoretical models shown in Figures 5 and 6. For an applied DEP signal of 1V, the T cells exhibited anti-field TWD motion between 40 kHz and 200 kHz. With an applied 2V DEP signal, the anti-field TWD range increased to 400 kHz and a co-field TWD window appeared above 5 MHz. As the magnitude of the 10 kHz DEP signal was progressively increased to 3 V and above, the TWD window became operative over the full range of measurements from 4 kHz to 60 MHz.

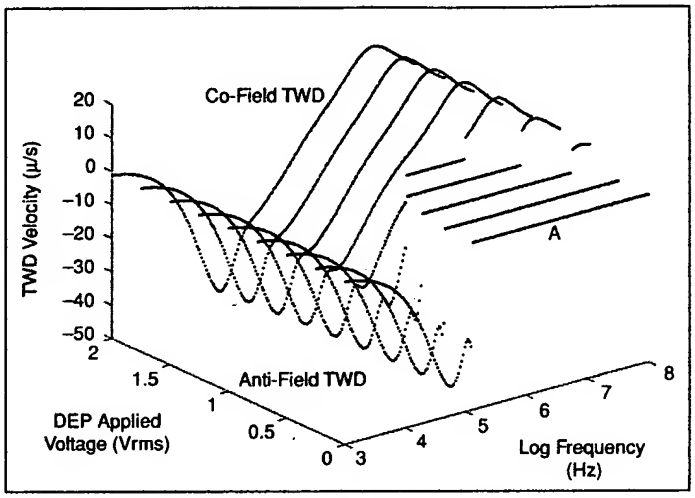

Fig. 6. Three-dimensional plot of the TWD frequency spectrum for T cells as a function of increasing magnitude of a superimposed 10 kHz DEP signal. Region "A" corresponds to the frequency range where cells are attracted to the electrodes and either remain stationary or exhibit unstable motions.

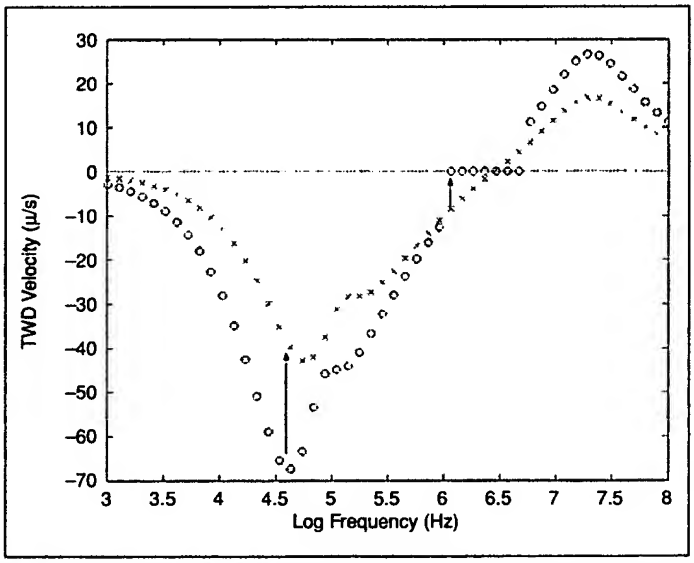

Fig. 7. The TWD frequency spectra for T cells (x) and monocytes (o), modeled for the case of a superimposed DEP signal. The TWD signal is set at 1 V(rms) and the DEP signal at 10 kHz, 1.06 V(rms). At 40 kHz the T cells and monocytes travel at velocities of 38 and 64 $\mu m \cdot s^{-1}$, respectively. At 1.3 MHz the T cells travel at 9 $\mu m \cdot s^{-1}$, while the monocytes are trapped on the electrodes.

Sequentially captured images are shown in Figure 9 of the TWD responses of T lymphocytes suspended above an array of interdigitated microelectrodes. Three separate signals have been applied to the electrodes: a 30 kHz, 3V DEP signal; a 75 kHz, 2.8V TWD signal; and a 350 kHz, 2.8V TWD signal. The quadrature phases of the TWD voltage signals were such that the two generated traveling fields acted against each other. Close inspection of Figure 9 reveals that there are three modes of behavior: a small number of cells remain stationary; some cells move to the right, while others move to the left. This behavior is consistent with the cells responding according to their phase of the cell cycle. In previous work [14] we have shown that, as T cells progress from the G_1 phase of their cell cycle through the S to the G_2/M phases, the DEP_{XO} values become progressively smaller. This reflects an increase in cell size, together with an increase in the complexity of the cell membrane topography as described by the extent of microvilli, molecular blebs, and membrane folding, for example. Basically, cells in the G_1 phase have, on average, a slightly smaller membrane electrical capacitance than cells at a later stage in the cell cycle [14]. This fact enables cells to be separated by TWD, according to cell cycle phase, as shown in Figure 9.

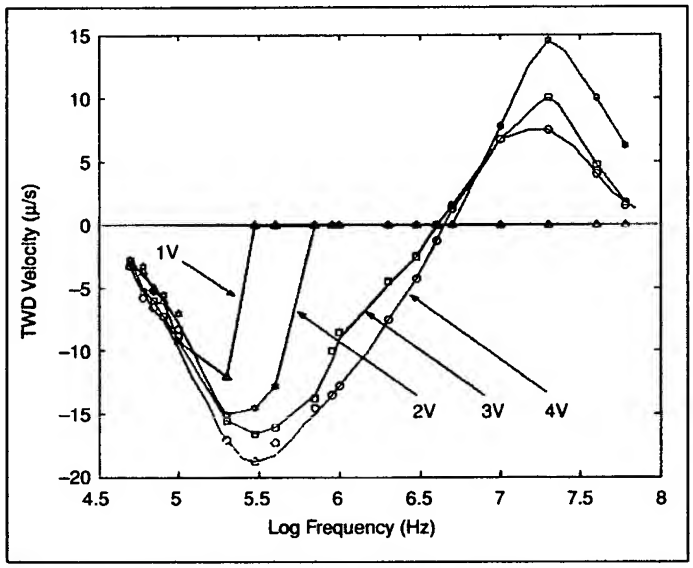

Fig. 8. The TWD response exhibited by T cells as a function of the magnitude of a superimposed 10 kHz DEP signal. As the magnitude of the DEP signal is progressively increased from 1 V(rms), the frequency window is increasingly extended as predicted by the theoretical models shown in Figures 5 and 6.

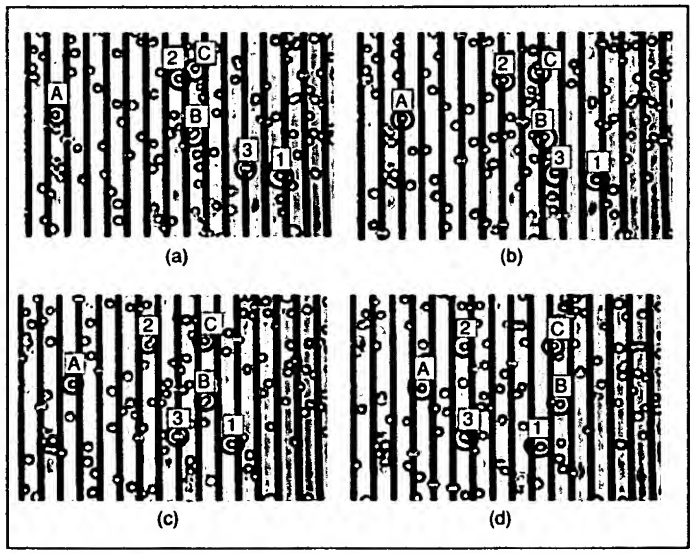

Fig. 9. Sequentially captured images of T cells, suspended above an array of interdigitated electrodes, moving under the influence of superimposed DEP and TWD signals. A subpopulation of cells (e.g., A, B, C) move to the right, while others (e.g., 1, 2, 3) move to the left, according to their cell cycle stage. The medium conductivity is 40 $mS \cdot m^{-1}$.

In another series of experiments, T cells and monocytes were mixed in a suspending medium of conductivity 40 $mS \cdot m^{-1}$. The separation of these cells by Superposition-TWD is shown in Figures 10 and 11. The sequence of events begins in Figure10, showing how cells moving in opposite directions are directed into separate paths as a result of the serpentine geometry of the electrode elements [17]. This reduces steric hindrance effects and also allows fluxes of different cell types to move freely and separately in opposite directions. Pure fractions of each cell type can be collected at specific sites along the TWD electrode tracks, as shown in Figure 11. These separations of T cells and monocytes were achieved by applying a 30 kHz, 2.6 V, DEP signal with two counter-traveling TWD signals, each of magnitude 2.8 V and frequencies of 75 kHz and 350 kHz, respectively. Separation of mixtures of T cells and monocytes by superposition TWD can be achieved without labeling the different cell types. However, in order to verify that efficient separation had occurred, the results shown in Figures 10 and 11 were obtained by tagging the T cells with a CD2-FITC (green fluorescent) antibody and the monocytes with a CD33-phycoerythrin (red fluorescent) antibody.

Discussion and Conclusions

Previous descriptions of TWD [2]–[12] describe the situation where a single voltage signal, of tunable frequency and quadrature phases, is applied to a microelectrode track. TWD can then be observed over a relatively restricted range of frequency, corresponding to where the vertical component of the generated dielectrophoretic force is such as to levitate particles above the electrode plane, and where the horizontal, phase nonuniformity component of this force is sufficient to induce translational motion of these particles along the electrode track. For a mixture of cell types, or of cells of differing physiological states, fractionation of these cells can be achieved if the electrode track is of sufficient length. The usual situation observed is that different cell types

Measurement of a superposition TWD response across the full frequency range will provide the same information as the electrorotation response plus the advantage that translational movement is much easier to detect and quantify.

exhibit the same sense of TWD motion, with a maximum difference of the order 10 $\mu m \cdot s^{-1}$ between the mean velocities of the individual velocity distributions at an optimum fixed TWD frequency. As a result of biological variability, there is usually an overlap of velocity distributions for different cell types. Electrode track lengths of at least 2 cm are normally required to achieve separation of useful numbers of cells into relatively pure fractions. This equates, in terms of Figure 1, to an array of at least 1,000 interdigitated electrode elements (mark-space ratio of 10 μm) and the accompanying challenges of microfabrication and the electrical addressing of individual electrode elements.

We have described a new approach, termed Superposition-TWD, whereby one or more DEP and TWD signals are applied together. The effect of such superposition of signals is to change the levitation height (Figure 4) of the particles above the electrode plane, and in so doing to alter the range of frequencies over which TWD occurs (Figures 6–8). The results shown in Figures 6–8 were achieved by adding a 10 kHz signal to the TWD signal. This imposed an additional cell levitation force on the cells and resulted in a broadening of the TWD frequency window. If a 1 MHz DEP signal had been chosen, for example, then, as shown in Figure 2, the polarizability parameter Re(m) has a positive value and this would introduce a force that attracts the cells to the electrodes. Thus, the levitation height can be carefully controlled so as to either widen or narrow the TWD frequency window. Narrowing the TWD window can result in the trapping of one type of particle on the electrodes, while enabling a second type of particle to be removed by TWD to differing levels of separation purity or efficiency. Widening the TWD window to the full range of available frequencies can extend the separation criteria available for exploitation, to cover differences in cell membrane morphology, integrity, and surface charge, for example (at the lower frequencies), or aspects of the cell interior associated with the endoplasmic reticulum or differences in nucleus-cytoplasm volume ratio (at the higher frequencies).

Particularly useful results can be produced by applying two or more TWD signals. Appropriate choices of TWD signal strengths and frequencies, as well as the senses of the applied quadrature phase sequences, can result in cells of different type or physiological state traveling in opposite directions (Figures 9 and 10). This provides significant advantages over previously described TWD methods and can result in improved levels of attainable sensitivity and purity of cell separations on shorter electrode tracks (e.g., 0.4 rather than 2.0 cm).

Finally, apart from cell-separation applications, this new method can be used to characterize cells and to monitor physiological changes occurring on exposure to chemical agents, for example. The ability to fully extend the frequency window available for TWD studies offers an alternative method to electrorotation for characterizing cells.

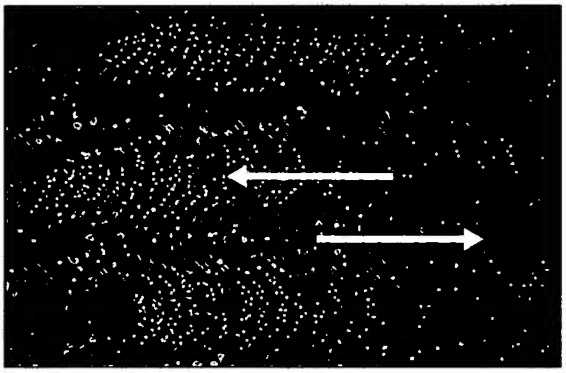

Fig. 10. The separation of T cells and monocytes from a mixture using superposition TWD. The serpentine geometry of the electrodes enables T cells (traveling to the left) to follow unimpeded and separate paths to those of the monocytes (moving right). The velocities of most cells fall within the range of 5–15 μm/s.

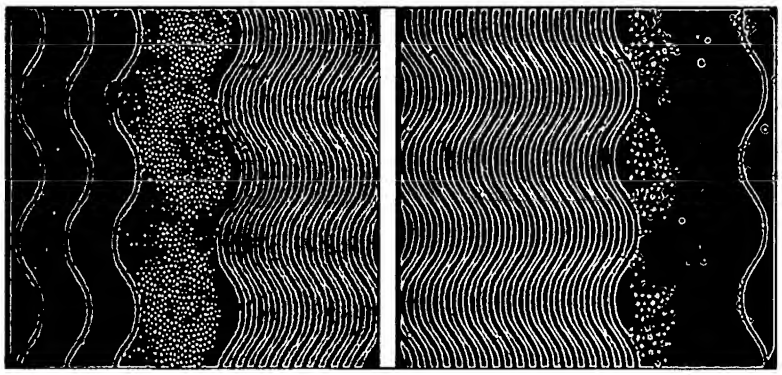

Fig. 11. T cells collecting to the left and monocytes to the right of the electrode array shown in Figure 10. To verify their separation, the T cells were labeled with a CD33-phycoerythrin (red fluorescent) marker and the monocytes with a CD2-FITC (green fluorescent) marker.

Since the time of its initial development [18], the theoretical and experimental aspects of cell electrorotation have been extended in several laboratories (see [9] and references cited therein) and shown to be a sensitive method for monitoring the physiological state of cells. The electrorotation effect shares with TWD the property of being dependent on the frequency variation of the polarizability factor Im(m). However, conventional TWD is observable over only a narrow frequency range, while the electrorotation effect can be observed over the full range of frequencies. Measurement of a superposition TWD response across the full frequency range will therefore provide the same information as the electrorotation response. Furthermore, there is the added advantage that translational movement is much easier to detect and quantify than the rotation of a cell. Determining the electrorotation rate of bacteria and viruses, for example, is particularly challenging, whereas the TWD motions of such particles can readily be quantified.

Acknowledgments

Early experiments of superposition TWD were performed by Gary M. Lock at the University of Wales, Bangor, during his Ph.D studies funded by a BBSRC research studentship and the National Foundation for Cancer Research. We thank Brenda Kusler and Cathy Carswell-Crumpton for their assistance with cell culture and flow cytometry.

Ronald Pethig received a Ph.D. degree in electrical engineering and a D.Sc. in biomolecular electronics from the University of Southampton, and a Ph.D. in chemistry from the University of Nottingham. He cofounded Aura BioSystems Inc. in 1998 and currently serves as vice-president, technology. Prior to founding Aura he was director of the Institute of Molecular and Biomolecular Electronics at the University of Wales, Bangor, and holds a personal chair in the School of Informatics. His honors include the joint Innovation Prize of the Institutes of Electrical and Mechanical Engineering and the British Design Council (1988), the 1994 Innovation Awards of the Institute of Physical Sciences in Medicine and the Biological Engineering Society, and in 2001 he became the first recipient of the Herman P. Schwan Award for work in biodielectrics.

Mark S. Talary received the B.Eng. degree in electronic engineering in 1988, the M.Eng. in electronic engineering in 1989, and the Ph.D. degree in biophysics in 1994 from the University of Wales, Bangor, U.K. During postdoctorial work he developed new biotechnological applications for dielectrophoresis, including work on cell separations in collaboration with the University of Wales, College of Medicine, Cardiff, in 1995. In 2000 he joined Aura BioSystems, Inc., San Jose, California, to work on industrial applications of dielectrophoresis.

Richard S. Lee received the B.Eng. degree in electronic engineering in 1993 and the Ph.D. degree in biophysics in 1997 from the University of Wales, Bangor, U.K. During postdoctorial work on a Leverhulme Research Fellowship he developed new imaging techniques for ac electrokinetic systems, and in collaboration with Industrial Research Ltd, New Zealand, he studied elution of bioparticles using permittivity gradients. In 2000 he joined Aura BioSystems, Inc. San Jose, California, to work on industrial applications of dielectrophoresis.

Address for Correspondence: Ronald Pethig, School of Informatics, University of Wales, Dean Street, Bangor, Gwynedd LL57 1UT, UK. E-mail: r.pethig@aurabiosys.com.

References

[1] S. Masuda, M. Washizu, and I. Kawabata, "Movement of blood cells by nonuniform traveling field," *IEEE Trans. Ind. Applicat.*, vol. 24, pp. 214–222, March/April 1988.

[2] R. Hagedorn, G. Fuhr, T. Müller, and J. Gimsa, "Travelling wave dielectrophoresis of microparticles," *Electrophoresis*, vol. 13, pp. 49–54, 1992.

[3] Y. Huang, J.A. Tame, and R. Pethig, "Electrokinetic behaviour of colloidal particles in traveling electric fields: studies using yeast cells," *J. Phys. D: Appl. Phys.*, vol. 26, pp. 1528–1535, 1993.

[4] X.-B. Wang, Y. Huang, F.F. Becker, and P.R.C. Gascoyne, "A unified theory of dielectrophoresis and traveling wave dielectrophoresis," *J. Phys. D: Appl. Phys.*, vol. 27, pp. 1571–1574, 1994.

[5] M.P. Hughes, R. Pethig, and X.-B. Wang, "Dielectrophoretic forces on particles in traveling electric fields", *J. Phys. D: Appl. Phys.*, vol. 29, pp. 474–482, 1996.

[6] H. Morgan, A.G. Izquierdo, D. Bakewell, N.G. Green, and A. Ramos, "The dielectrophoretic and traveling wave forces generated by interdigitated electrode arrays: analystical solution using Fourier series," *J. Phys. D: Appl. Phys.*, vol. 34, pp. 1553–1561, 2001.

[7] M.S. Talary, J.P.H. Burt, J.A. Tame, and R. Pethig, "Electromanipulation and separation of cells using traveling electric fields," *J. Phys. D: Appl. Phys.*, vol. 29, pp. 2198–2203, 1996.

[8] X.-B. Wang, Y. Huang, X. Wang, F.F. Becker, and P.R.C. Gascoyne, "Dielectrophoretic manipulation of cells in spiral electrodes," *Biophysical J.*, vol. 72, pp. 1887–1899, 1997.

[9] A.D. Goater, J.P.H. Burt, and R. Pethig, "A combined traveling wave dielectrophoresis and electrorotation device: applied to the concentration and viability determination of *Cryptosporidium*," *J. Phys. D: Appl. Phys.*, vol. 30, pp. L65–L69, 1997.

[10] H. Morgan, N.G. Green, M.P. Hughes, W. Monaghan, and T.C. Tan, "Large-area traveling-wave dielectrophoresis particle separator," *J. Micromech. Microeng.*, vol. 7, pp. 65–70, 1997.

[11] R. Pethig, J.P.H. Burt, A. Parton, N. Rizvi, M.S. Talary, and J.A. Tame, "Development of biofactory-on-a-chip technology using excimer laser micromachining," *J. Micromech. Microeng.*, vol. 8, pp. 57–63, 1998.

[12] J.P.H. Burt, R. Pethig, and M.S. Talary, "Microelectrode devices for manipulating and analyzing bioparticles," *Trans. Inst. MC*, vol. 20, pp. 82–90, 1998.

[13] G.M. Lock and R. Pethig, "Travelling wave dielectrophoretic apparatus and method," International Patent Application: WO 01/05514 A1, January 25, 2001.

[14] R. Pethig, V. Bressler, C. Carswell-Crumpton, Y. Chen, L. Foster-Haje, M.E. Garcia-Ojeda, R.S. Lee, G.M. Lock, M.S. Talary, and K.M. Tate, "Dielectrophoretic studies of the activation of human T lymphocytes using a newly developed cell profiling system," *Electrophoresis*, vol. 23, pp. 2057–2063, 2002.

[15] G.H. Markx, R. Pethig, and J. Rousselet, "The dielectrophoretic levitation of latex beads, with reference to field-flow fractionation," *J. Phys. D: Appl. Phys.*, vol. 30, pp. 2470–2477, 1997.

[16] J. Yang, Y. Huang, X.-B. Wang, F.F. Becker, and P.R.C. Gascoyne, "Cell separation on microfabricated electrodes using dielectrophoretic/gravitational field-flow fractionation," *Anal. Chem.*, vol. 71, pp. 911–918, 1999.

[17] G.M. Lock and R. Pethig, "Dielectrophoretic apparatus and method," International Patent Application: WO 01/05512 A1, Jan. 25, 2001.

[18] W.M. Arnold and U. Zimmermann, "Electrorotation: Developments of a technique for dielectric measurements on individual cells and particles," *J. Electrostatics*, vol. 21, pp. 151–191, 1988.